

In the case of SrO the temperature dependence of the evolution of Sr suggests that the dissociation at low energies is a surface reaction while at high energies a reaction within the solid occurs. Additional support for this suggestion is provided by the variation of the oxygen evolution with the energy of the incident electrons. The release of oxygen from materials bombarded with electrons having energies near 5-electron volts, which has frequently been ascribed to a dissoci-

ation process, appears rather to result from a desorption of a gas film.

ACKNOWLEDGMENTS

The authors wish to acknowledge their appreciation to Professor A. J. Dekker for many helpful discussions and suggestions. They are also indebted to W. T. Peria for a number of suggestions concerning the investigation and to B. V. Haxby for his continuing interest and assistance in the preparation of the manuscript.

PHYSICAL REVIEW

VOLUME 106, NUMBER 4

MAY 15, 1957

Opto-Electronic Properties of Mercuric Iodide

RICHARD H. BUBE

RCA Laboratories, Radio Corporation of America, Princeton, New Jersey

(Received February 8, 1957)

The optical and photoelectrical properties of mercuric iodide crystals and layers have been investigated, particularly as affected by the phase transformation from tetragonal (low-temperature form) to orthorhombic (high-temperature form) which occurs at 400°K. The largest temperature coefficient for band-gap variation of any known material is found for the orthorhombic form: -24×10^{-4} ev/degree. The following phenomena are discussed: (1) location and temperature dependence of absorption edge by measurements of transmission, reflectivity, and photoconductivity response spectra; (2) temperature dependence of dark current; (3) electrode effects in photoconductivity; (4) variation of dark current and photocurrent through the phase transformation; (5) thermally-stimulated-currents; (6) variation of photocurrent with voltage, light intensity, and temperature. Temperature-quenching of photoconductivity in HgI₂ crystals can be described by means of the same analysis as has been applied to various $A^{IV}B^{VI}$ photoconductors, giving a location of 0.5 ev above the valence band for the "sensitizing" centers in HgI₂.

1. INTRODUCTION

MERCURIC iodide was one of the earliest materials to be investigated for photoconductivity. In 1903, it was shown¹ that HgI₂ could be used with gelatin to form a photographic emulsion. Other workers studied the spectral response and the mechanism of photoconductivity.²⁻⁴ Nix⁵ reported that the photosensitivity of HgI₂ crystals grown from ethyl alcohol solution was lost after about a year, as the crystals became polycrystalline, but could be restored by the application of a field. Putseiko⁶ studied photoconductivity and dye-sensitization phenomena in HgI₂. Chepur⁷ discussed the formation of melted-and-recrystallized layers, crystals grown from the melt, and crystals grown from acetone solution, together with their photoconductivity. The existence of excitons in HgI₂ has been indicated by Nikitine⁸ and by Gross⁹; Gross has also reported that the photosensitivity of the orthorhombic form of HgI₂

is about 0.1% of that of the tetragonal form. A study of the phase-transformation kinetics has been reported by Newkirk¹⁰ for the transformation of the "red" tetragonal form of HgI₂ to the "yellow" orthorhombic form with increasing temperature at about 400°K; he has shown that the transformation consists of a shift of the (100) plane in the tetragonal form to the (110) plane in the orthorhombic form; the [001] direction is preserved.

The present investigation was motivated originally by interest in the effects of the phase transformation on the optical and photoelectrical properties of HgI₂. As the work progressed, however, this investigation was broadened to include many of the semiconducting and photoconducting characteristics of HgI₂: temperature dependence of the band-gap; low-temperature luminescence; electrode problems; temperature dependence of dark current; dependence of photocurrent on voltage, light intensity, temperature, and wavelength; and thermally stimulated currents.

2. MATERIAL PREPARATION

Samples of HgI₂ were measured (a) in microcrystalline (powder) form, (b) as sintered layers produced by vapor deposition, (c) as melted and recrystallized polycrystalline layers, (d) as crystals grown from the

¹ Lупpo-Cramer, *Eder's Jahrbuch* (1903), p. 24.

² G. Athanasiu, *Compt. rend.* **176**, 1389 (1923).

³ M. Volmer, *Z. wiss. Phot.* **16**, 152 (1916).

⁴ F. Kampf, *Physik. Z.* **23**, 420 (1922).

⁵ F. C. Nix, *Phys. Rev.* **47**, 72 (1935).

⁶ E. K. Putseiko, *Izvest. Akad. Nauk, S.S.S.R., Ser. Fiz.* **16**, 34 (1952); E. K. Putseiko and A. N. Terenin, *Doklady Akad. Nauk, S.S.S.R.* **70**, 401 (1950).

⁷ D. V. Chepur, *Zhur. Tekh. Fiz.* **25**, 2411 (1955).

⁸ S. Nikitine, *Compt. Rend.* **240**, 1324 (1955).

⁹ E. F. Gross, *Zhur. Tekh. Fiz.* **25**, 1661 (1955).

¹⁰ J. B. Newkirk, *Acta Metallurgica* **4**, 316 (1956).

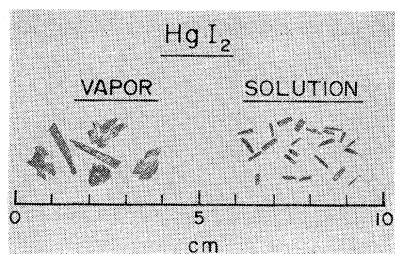


FIG. 1. Photograph of HgI_2 crystals grown from the vapor-phase and from acetone solution.

vapor phase, and (e) as crystals grown from acetone solution.¹¹

2.1. Microcrystalline (Powder) Form

Eimer and Amend *CP* HgI_2 was used in measurements of band gap by diffuse reflectivity.

2.2. Sintered Layers

Sintered layers of HgI_2 were prepared by heating HgI_2 powder in a platinum dish covered by a quartz plate to a temperature such that the powder vaporized and deposited on the quartz plate. The layer thus formed was separated from the quartz plate after cooling; the surface of the layer next to the plate formed a smooth sintered layer.

2.3. Melted and Recrystallized Layers

HgI_2 powder was placed between two quartz plates and heated to such a temperature that the powder melted. Upon cooling, the layer recrystallized; the plates were separated to leave the layer deposited predominantly on one of the plates.

2.4. Vapor Phase Crystals

HgI_2 powder was heated in the bottom of a firing tube to between 500° and 600°C for about 10 min.

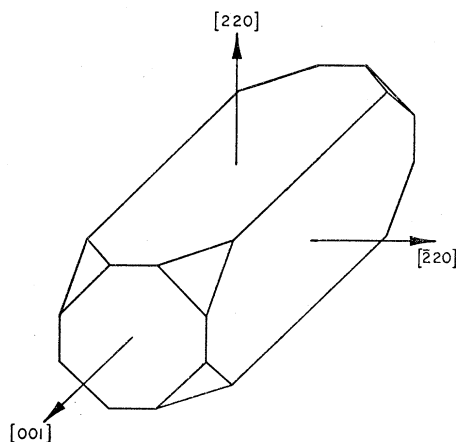


FIG. 2. Schematic representation of a tetrahedral HgI_2 crystal grown from solution, showing the crystal directions of the major axes.

¹¹ Preparations (c), (d), and (e) by S. M. Thomsen.

Crystals deposited from the vapor phase formed in the upper unheated portion of the tube.

2.5. Solution-Grown Crystals

A saturated solution of HgI_2 powder in acetone was prepared. The solution was allowed to stand in lightly-covered tall cylindrical vessels for several weeks. As the acetone evaporated, crystals of HgI_2 deposited in the bottom of the vessels. One lot of crystals was prepared from a solution containing 75% HgI_2 and 25% HgCl_2 by weight.

The methods of preparation used are such that only the solution-grown crystals have not passed through a phase transformation. Several solution-grown crystals were heated above the transformation temperature and then recooled.

Figure 1 is a photograph showing several typical vapor-phase-grown crystals and solution-grown crystals. The general morphology of the solution-grown crystals is indicated in Fig. 2. X-ray analysis¹² indicated the crystal directions shown in Fig. 2, and showed that the solution-grown HgI_2 crystals had some good crystalline portions; definite evidence of x-ray spot breakup, how-

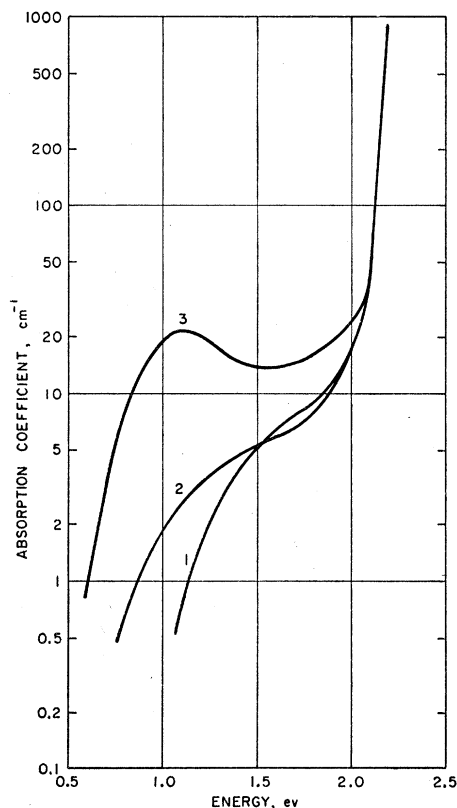


FIG. 3. Transmission spectra at room temperature for (1) a solution-grown crystal of tetrahedral HgI_2 , (2) same as (1) after having passed through a transformation cycle, (3) melted-and-recrystallized layer.

¹² X-ray analysis by J. White.

ever, indicated lack of uniform crystallinity. Solution-grown crystals which had been heated above the transformation temperature and re-cooled showed only slight evidence of crystallinity by x-ray analysis.

3. TRANSMISSION SPECTRA

Transmission spectra were measured¹³ for a solution-grown crystal, a solution-grown crystal which had been heated above the transformation temperature and re-cooled, and a melted-and-recrystallized layer. The results are shown in Fig. 3. The exponential portion of the variation of absorption constant with energy sets in at about 2.11 eV at room temperature. This corresponds to an absorption-edge wavelength of 5870 Å; calculation of the ratio of the fourth power of the geometric mean of the refractive indices (2.748 and 2.455;¹⁴ geometric mean = 2.597) to the absorption-edge wavelength gives a value of 77.5 for Moss's constant,¹⁵ which is almost exactly the average value of 77 proposed to hold for a variety of photoconductors. An additional absorption peak at 1.1 eV is found for the melted-and-recrystallized layer; corresponding photoconductivity was not observed.

4. REFLECTIVITY SPECTRA

Diffuse-reflectivity spectra were measured on powder HgI_2 to determine the variation of the band-gap with temperature and transformation of crystal form. Figure 4 shows the reflectivity spectra at room temperature obtained successively for the same sample before a transformation and after a transformation (the sample now being in sintered-layer form), together with the reflectivity of the orthorhombic form at 400°K. The

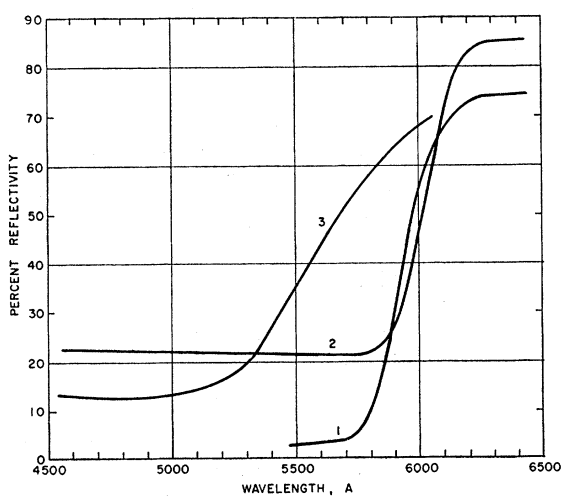


FIG. 4. Diffuse reflectivity spectra for (1) powder tetr.- HgI_2 at room temperature, (2) sintered layer of tetr.- HgI_2 formed from the vapor-phase from material of (1), at room temperature, (3) powder orthorhomb.- HgI_2 at 403°K.

¹³ Measured by W. E. Spicer.

¹⁴ N. A. Lange's *Handbook of Chemistry* (Chemical Rubber Publishing Company, Cleveland, 1946), sixth edition, p. 873.

¹⁵ T. S. Moss, Proc. Phys. Soc. (London) **B63**, 167 (1950).

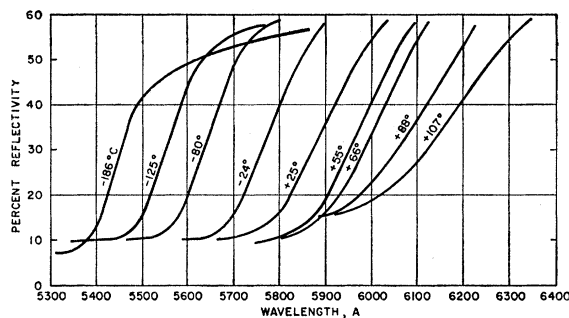


FIG. 5. Diffuse reflectivity spectra for powder tetr.- HgI_2 as a function of temperature.

determination of band-gap from diffuse-reflectivity spectra has been carried out according to the suggestion of Fochs¹⁶; the wavelength for the onset of the linear portion of greatest slope, associated with the onset of an exponential drop of absorption coefficient, is chosen as the absorption edge. Use of this criterion gives an absorption edge at 5840 Å (2.12 eV) for tetr.- HgI_2 at room temperature and an absorption edge at 5350 Å (2.31 eV) for orthorhomb.- HgI_2 at 400°K. The sintered layer shows high wavelength-independent reflectivity at low wavelengths (specular reflection component present) because of the shiny nature of the sintered surface. The apparent absorption edge is 5920 Å; the difference between this value and that obtained previously for the powder is probably not significant.

4.1. Temperature Dependence of Band Gap for Tetr.- HgI_2

The reflectivity spectra for tetr.- HgI_2 are given in Fig. 5 for various temperatures between 87° and 380°K. The absorption edge shifts from 5410 Å (2.29 eV) at 87°K to 6105 Å (2.03 eV) at 380°K.

4.2. Temperature Dependence of Band Gap for Orthorhomb.- HgI_2

Tetr.- HgI_2 was heated above the transformation temperature to convert it to the orthorhombic form; the latter was rapidly quenched in liquid nitrogen to preserve the orthorhombic form at low temperatures. Figure 6 shows the reflectivity spectra for orthorhomb.- HgI_2 between 90° and 204°K. The edge loses sharpness very rapidly upon heating, and above 204°K the orthorhombic form starts to convert spontaneously to the tetragonal form. The absorption edge of the orthorhomb.- HgI_2 shifts from 4075 Å (3.05 eV) at 90°K to 4440 Å (2.80 eV) at 204°K.

4.3. Reflectivity Spectra When Both Tetr.- HgI_2 and Orthorhomb.- HgI_2 Are Present

As mentioned in the previous section, the quenched orthorhombic form starts to convert to the tetragonal

¹⁶ P. D. Fochs, Proc. Phys. Soc. (London) **B69**, 70 (1956).

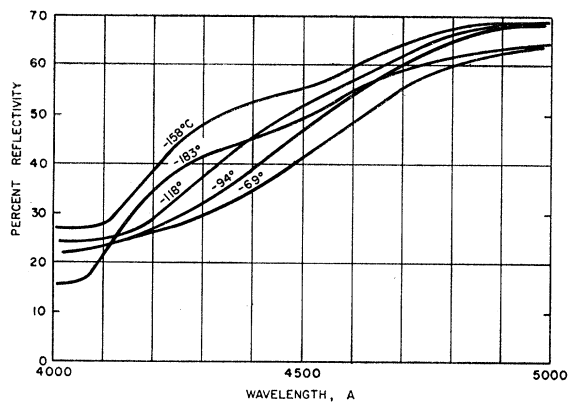


FIG. 6. Diffuse reflectivity spectra for powder orthorhomb.- HgI_2 as a function of temperature.

form above 204°K. Reflectivity spectra taken in the range between 204° and 256°K, shown in Fig. 7, show the presence of both the orthorhombic edge and the tetragonal edge. The relative magnitude of the reflectivity plateau between 4800 Å and 5500 Å is a measure of the relative proportions of the two phases present.

The temperature dependence of band-gap, as determined from reflectivity spectra is summarized in Fig. 8. Curve 2 summarizes the data from Fig. 5, showing that the temperature coefficient for variation of the band-gap in tetr.- HgI_2 is about -7×10^{-4} eV/degree between 100° and 200°K and about -14×10^{-4} eV/degree between 330° and 400°K. Curve 1 summarizes the data on the location of the absorption edge from Fig. 4 and Fig. 6 for the orthorhomb.- HgI_2 . The straight line indicated by the measured points at low temperatures extrapolates linearly to the measured point at 400°K, giving a temperature coefficient of -24×10^{-4} eV/degree.

These temperature coefficients are much larger than any that have been reported to date and present an interesting problem for theoretical investigation. Temperature coefficients for such materials as germanium, silicon, cadmium sulfide, zinc sulfide, zinc selenide,

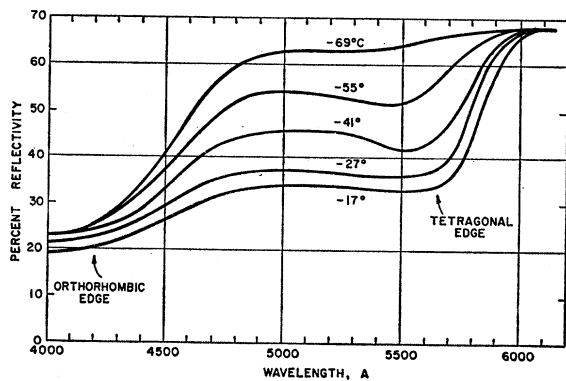


FIG. 7. Diffuse reflectivity spectra for powder HgI_2 , showing the presence of both crystalline forms between -69° and -17°C .

cadmium selenide, and cadmium telluride¹⁷⁻¹⁹ are of the order of -3×10^{-4} to at most -8×10^{-4} eV/degree. It has been shown for materials of this type that variation of band-gap because of crystal dilation can account for only a small fraction of the observed shift.^{20,21} Theoretical discussions, such as that by Fan,²² indicate that consideration of temperature-excitation of lattice vibrations can give values of temperature coefficient which are of the same order of magnitude as those observed, but still in general somewhat smaller.

A summary of the temperature dependence of band-gap in tabular form is given in Table I.

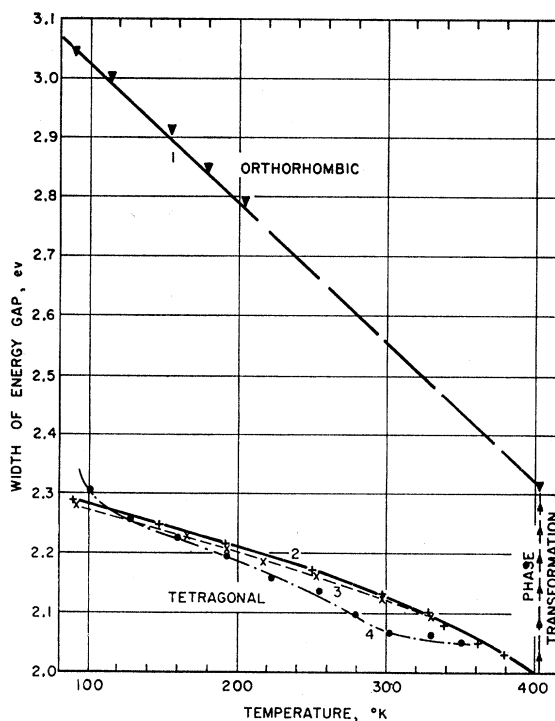


FIG. 8. Width of the energy gap as a function of temperature for (1) orthorhomb.- HgI_2 , from reflectivity; (2) tetr.- HgI_2 , from reflectivity; (3) tetr.- HgI_2 , melted-and-recrystallized layer, from spectral response of photoconductivity; (4) tetr.- HgI_2 , solution-grown crystal, from spectral response of photoconductivity.

5. LUMINESCENCE EMISSION

Luminescence emission was observed for the tetr.- HgI_2 form at liquid nitrogen temperature. The emission spectrum obtained from excitation of vapor-phase-grown tetr.- HgI_2 crystals by 3650-Å ultraviolet is shown in Fig. 9. Three emission bands are found with maxima at 5360 Å, 5675 Å, and 6200 Å; their intensities are in the ratio of 1:10:45, respectively. The lowest wave-

¹⁷ M. L. Schultz and G. A. Morton, Proc. Inst. Radio Engrs. 43, 1819 (1955).

¹⁸ R. H. Bube, Phys. Rev. 98, 431 (1955).

¹⁹ R. H. Bube, Proc. Inst. Radio Engrs. 43, 1836 (1955).

²⁰ G. Hoehler, Ann. Physik 4, 371 (1949).

²¹ W. Shockley and J. Bardeen, Phys. Rev. 77, 407 (1950).

²² H. Y. Fan, Phys. Rev. 78, 808 (1950).

length band corresponds approximately to edge emission; the extrapolated absorption edge at 77°K from curve 2 of Fig. 8 is 5390 Å. All luminescence is thermally quenched upon only a slight warming above 77°K. The emission is almost identical with that reported by Sieskind²³ who reported emission bands at 77°K for HgI₂ at 5355 Å, 5600 Å, and 5925–6500; Sieskind attributed the 5355-Å band to excitons and suggested that the other two bands were due to either excitons or impurities.

6. ELECTRODES

The choice of suitable electrodes posed a major problem with HgI₂, principally because of reaction between common electrode materials and the HgI₂. Silver, indium, and gallium electrodes were all tried, but reaction between the metal and the HgI₂ occurred,

TABLE I. Temperature dependence of band gap.

Reflectivity, tetr.-HgI ₂			Reflectivity, orthorhomb.-HgI ₂		
T°K	λ, Å	E _g , ev	T°K	λ, Å	E _g , ev
87	5410	2.29	90	4075	3.045
148	5510	2.25	115	4125	3.005
193	5595	2.215	155	4250	2.915
249	5715	2.17	179	4350	2.85
298	5820	2.13	204	4440	2.795
328	5905	2.10	403	5350	2.315
339	5960	2.08			
361	6045	2.05			
380	6105	2.03			

Photoconductivity, solution-grown tetr.-HgI ₂			Photoconductivity, melted-and-recrystallized tetr.-HgI ₂		
T°K	λ, Å	E _g , ev	T°K	λ, Å	E _g , ev
102	5375	2.305	91	5430	2.28
128	5500	2.255	128	5490	2.26
160	5575	2.225	166	5555	2.23
193	5650	2.195	194	5605	2.21
222	5750	2.155	218	5670	2.185
252	5810	2.135	252	5740	2.16
280	5910	2.095	298	5850	2.12
302	6000	2.065	330	5910	2.095
329	6020	2.06			
349	6050	2.05			

usually within minutes, causing permanent changes in the cell properties. Especially unusual properties were obtained in the case of silver; dark current increased by many orders of magnitude upon operation of the cell under illumination. When such a high-conductivity state had been reached, it was observed that illumination reduced the dark current, producing negative photoconductivity. This effect is probably analogous to that reported by Yamada²⁴ for a negative photoeffect in AgBr, resulting from quenching of ionic conductivity as a result of illumination.

To obtain electrodes which would be chemically non-reactive with HgI₂ and which would be stable enough to permit measurements as a function of temperature, graphite was chosen as the electrode material.

²³ M. Sieskind, *J. phys et radium* **17**, 821 (1956).

²⁴ K. Yamada, *Naturwiss.* **43**, 175 (1956).

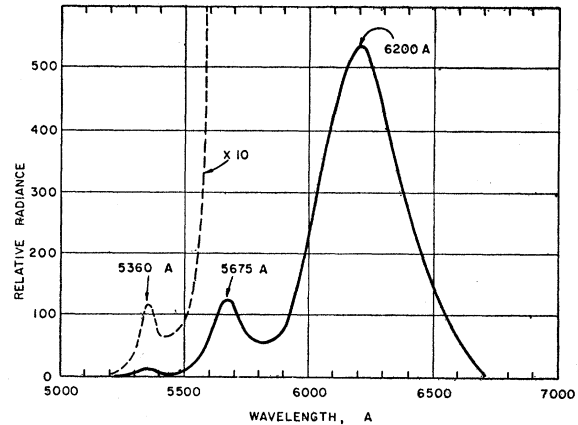


FIG. 9. Luminescence emission spectrum for excitation of vapor-phase-grown tetr.-HgI₂ crystals by 3650 Å ultraviolet at 77°K.

7. TEMPERATURE DEPENDENCE OF DARK CURRENT

The dark current was measured as a function of temperature for various samples of tetr.-HgI₂. The results for a solution-grown crystal, two vapor-phase-grown crystals, and a melted-and-recrystallized layer are shown in Fig. 10 (data obtained as continuous record on a recorder). The room-temperature dark conductivity for the samples measured is about 10⁻¹² (ohm cm)⁻¹. The slopes of the curves of Fig. 10 vary from 0.96 to 1.12 ev, with an average value of 1.04 ev. Assuming that this slope corresponds to one-half the band-gap, good agreement is found with the value of the band-gap determined optically. The data of Fig. 10 are therefore evidence that the dark conductivity

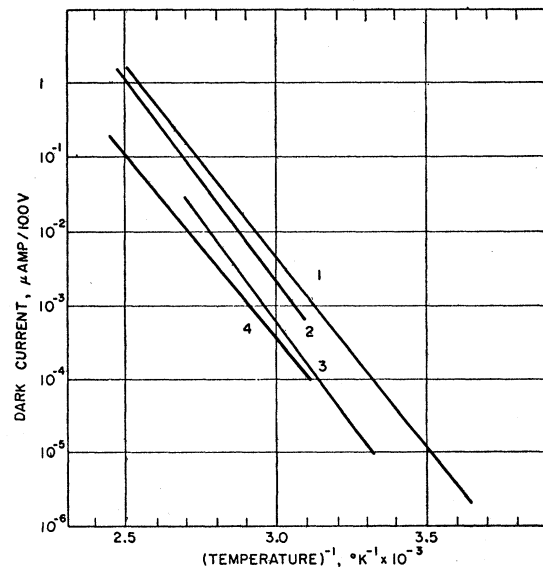


FIG. 10. Temperature dependence of dark current for (1) melted-and-recrystallized layer of tetr.-HgI₂, (2) and (3), vapor-phase-grown crystals of tetr.-HgI₂, (4) solution-grown crystal of tetr.-HgI₂.

corresponds to the intrinsic conductivity of HgI_2 and is not associated with impurities.

8. LIGHT-SPOT SCANNING OF CRYSTALS

To determine whether the photoconductivity observed when HgI_2 was illuminated was a uniform effect or was concentrated at one of the electrodes, the photocurrent in a solution-grown crystal was measured as a small spot of light (diameter less than $\frac{1}{10}$ of electrode spacing) was moved along the crystal. Measurements of response for several samples showed that photosensitivity was limited to a small region of the crystal at or near the cathode. Figure 11 illustrates the results for one crystal for both white light and green light. The apparent sensitivity of the crystal for white light at distances more than a few tenths of a millimeter from the cathode is probably caused by scattering of the weakly-absorbed red light, as indicated by the much smaller extent of sensitivity for the strongly-absorbed green light.

Voltage probing of the crystal also indicated a non-uniform potential distribution, with most of the potential drop at the cathode.

9. PHOTOCONDUCTIVITY RESPONSE SPECTRA

Photoconductivity was easily detectable with all tetr.- HgI_2 samples. The maximum photosensitivity found was about 10^3 to 10^4 microampere per lumen, cor-

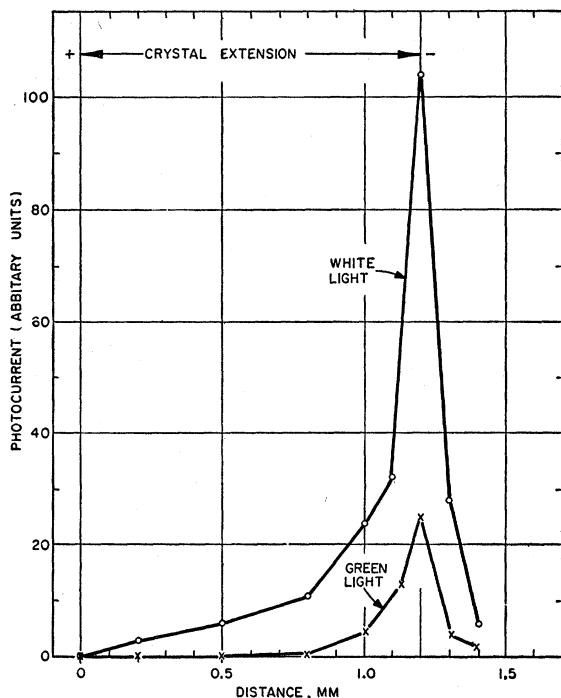


FIG. 11. Photocurrent for a solution-grown crystal of tetr.- HgI_2 as a function of the position of a small spot of light.

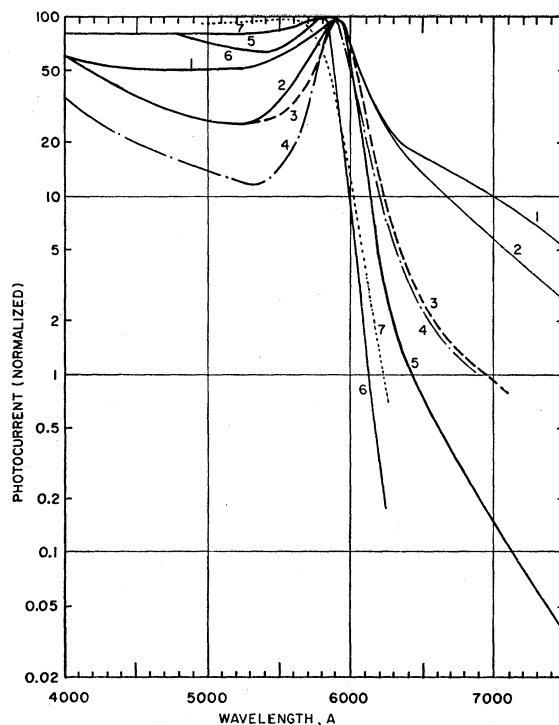


FIG. 12. Spectral response curves for photoconductivity in tetr.- HgI_2 : (1) solution-grown crystal, (2) same as (1) after having passed through a transformation cycle, (3) solution-grown crystal from solution containing 25% HgCl_2 , (4) vapor-phase-grown crystal, (5) sintered layer from vapor phase, (6) melted-and-recrystallized layer, (7) same as (6) after treatment in iodine vapor for 2 hours at 100°C . All samples give approximately the same photocurrent at room temperature; since samples (5), (6), (7) have about ten times the electrode length of the others, it indicates that (5), (6), (7) are about one-tenth as sensitive.

responding, respectively, to a specific sensitivity²⁵ of about 10^{-4} to 10^{-5} mho cm^2 per watt. The first figure in each case corresponds to the assumption of an effective crystal length equal to the electrode spacing, the second figure to an effective crystal length $\frac{1}{10}$ the electrode spacing.

9.1. Room Temperature Data

Photoconductivity response spectra for seven different forms of tetr.- HgI_2 are shown in Fig. 12. The magnitude of the response at long wavelengths beyond the absorption edge is greatest for the solution-grown crystal and least for the melted-and-recrystallized layer. The long-wavelength response may be attributed either to impurities which are removed by methods of preparation involving vaporization or melting, or to possible lack of stoichiometry in the solution-grown crystals. The melted-and-recrystallized layer is some-

²⁵ Specific sensitivity is defined as the measured conductance in mhos, multiplied by the square of the electrode spacing, and divided by the incident energy in watts. Specific sensitivity is independent of geometry, voltage, and light intensity, if the photocurrent varies linearly with voltage and light intensity. For sensitive photoconductors like CdS and CdSe, the specific sensitivity is about 10^{-1} to 1 mho cm^2 per watt.

what less sensitive than the solution-grown crystals, and the situation may well be analogous to that reported for "pure" CdS crystals²⁶ for which an increase in relative long-wavelength sensitivity was found to accompany an increase in overall sensitivity. There is no evidence that any appreciable porportion of HgCl₂ has been incorporated into the crystals grown from the solution containing 25% HgCl₂, but the presence of the HgCl₂ seems to have caused increased purity or stoichiometry of the growing HgI₂ crystals.

The curves in Fig. 12 have been corrected for photon flux assuming a linear variation of photocurrent with light intensity. The apparent negative slope of some of the curves for short wavelengths may be attributed to a variation of photocurrent with light intensity which is less rapid than linear.

9.2. Solution-Grown Crystal

The spectral response curves for a typical solution-grown crystal are shown in Fig. 13 at ten temperatures between 102°K and 349°K. The curves have not been normalized and thus the actual variation of photocurrent at any wavelength with temperature can be obtained from the data. This variation will be discussed in a later section (see Sec. 14). The following general observations may be made: (1) the prominence of the maximum at the approximate absorption edge is least

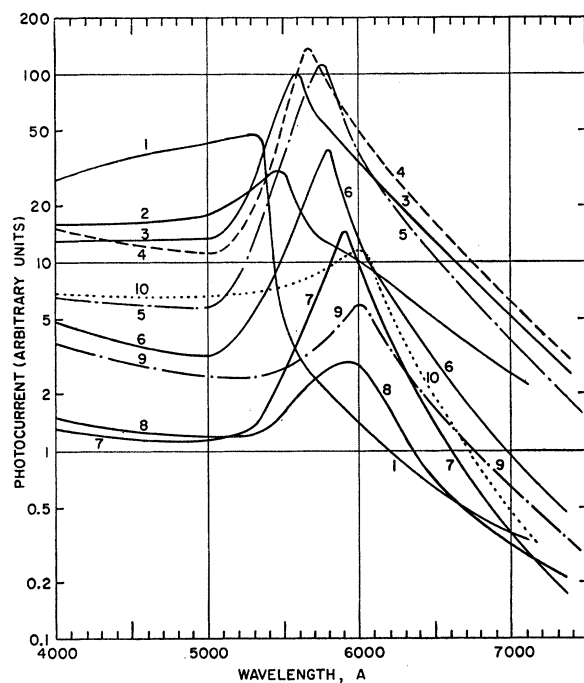


FIG. 13. Spectral response curves for a solution-grown tetr.-HgI₂ crystal as a function of temperature: (1) 102°K, (2) 128°K, (3) 160°K, (4) 193°K, (5) 222°K, (6) 252°K, (7) 280°K, (8) 302°K, (9) 329°K, (10) 349°K.

²⁶ R. H. Bube, Phys. Rev. **101**, 1668 (1956).

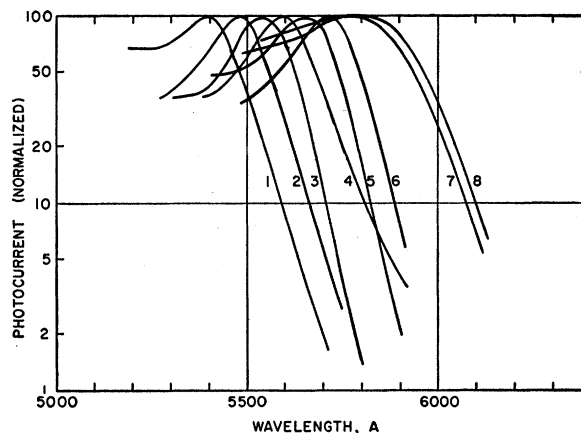


FIG. 14. Spectral response curves for a melted-and-recrystallized layer of tetr.-HgI₂ as a function of temperature: (1) 91°K, (2) 128°K, (3) 166°K, (4) 194°K, (5) 218°K, (6) 252°K, (7) 298°K, (8) 330°K.

at low temperatures and at high temperatures, reaching greatest prominence at about 223°K; (2) for wavelengths shorter than the absorption edge, the photocurrent shows a minimum with increasing temperature between 283° and 303°K with higher photocurrents at both low and high temperatures; (3) for wavelengths equal to or longer than the absorption edge, the photocurrent increases to a maximum at about 193°K, then decreases to a minimum at about 303°K, and then increases again.

The location of the absorption edge was estimated for each curve as the point of intersection of two straight lines, one drawn with slope of the photocurrent *vs* temperature curve just below the photocurrent maximum, and the other drawn with the slope of the photocurrent *vs* temperature curve just above the photocurrent maximum. The results are plotted as Curve 4 in Fig. 8. For all temperatures except the lowest, the maximum photosensitivity for this solution-grown crystal occurs for energies several hundredths of a volt smaller than the reflectivity-determined band-gap.

9.3. Melted-and-Recrystallized Layer

The data of Fig. 12 show that the long-wavelength cutoff in the photoconductivity response spectra of the melted-and-recrystallized layer is much sharper than that of the solution-grown crystal. It was believed, therefore, that the photosensitivity maximum for the melted-and-recrystallized layer would correspond more closely to the absorption edge determined by transmission or reflection. Such an expectation was realized. The response spectra are shown in Fig. 14 and the computed energies for photosensitivity maxima are plotted as Curve 3 of Fig. 8. For this layer, the photosensitivity maximum never lies more than a hundredth of a volt below the reflectivity-determined band-gap.

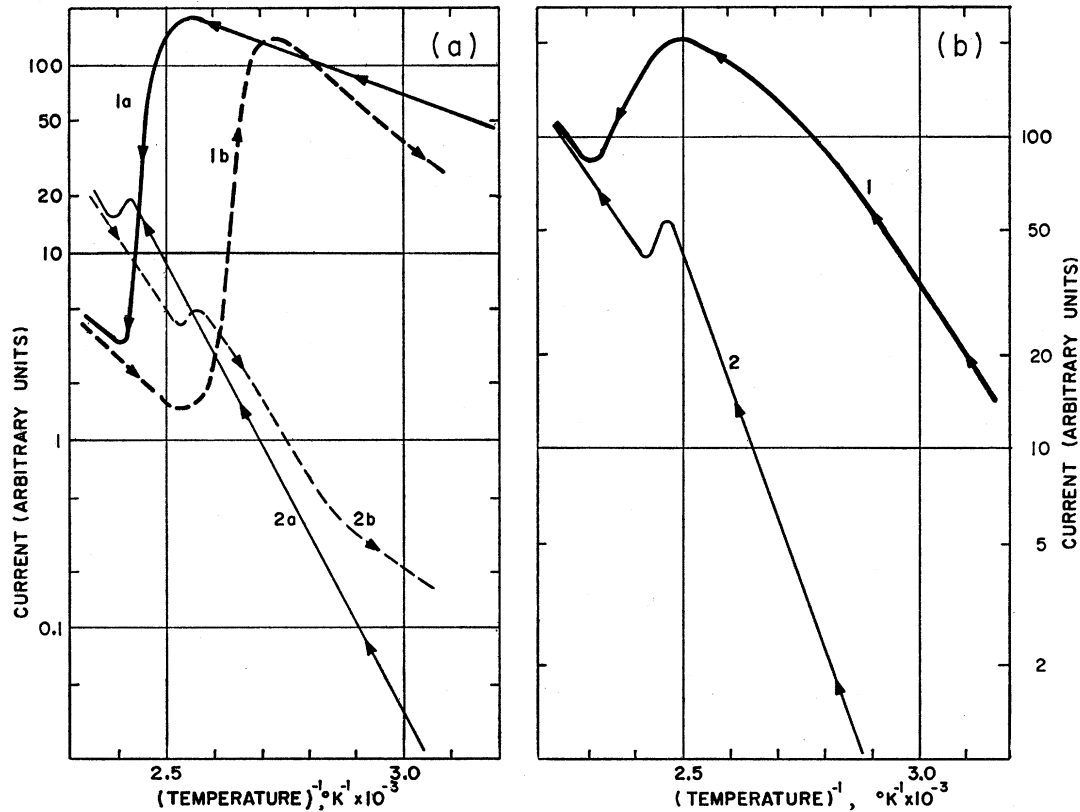


FIG. 15. (a) Variation of dark current (2a,2b) and photocurrent (1a,1b) as a function of temperature through the phase transformation, for uniform heating and illumination of a solution-grown HgI_2 crystal. (b) Variation of dark current (2) and total current under illumination (1) for a solution-grown HgI_2 crystal, as a function of temperature through the phase transformation, for a narrow slit of illumination on the center of the crystal, and for heating conditions such that one end of the crystal was raised above the transformation temperature before the other end.

10. EFFECT OF PHASE TRANSFORMATION ON DARK AND PHOTOCONDUCTIVITY

To determine the effect of the phase transformation on the dark-conductivity and photoconductivity of HgI_2 , a simple apparatus was constructed which permitted independent temperature-control of the two ends of a crystal. Using this apparatus, the crystal could be heated uniformly past the phase transformation, or one end of the crystal could be maintained at a temperature above the transformation temperature with the other end maintained below the transformation temperature, so that the transformation boundary could be moved down the crystal or stabilized at a particular location at will. Unfortunately, the phase transformation for HgI_2 is accompanied by the onset of rapid vaporization of the material, making prolonged measurements on a partially or totally transformed crystal impractical.

10.1. Solution-Grown Crystal

Figure 15(a) shows the temperature variation of the dark current and the photocurrent for a solution-grown HgI_2 crystal, for uniform illumination of the whole

crystal and uniform heating of both ends of the crystal. The phase transformation for heating occurs at a different temperature from that for cooling, both being somewhat removed from the theoretical temperature of 400°K , because of superheating and supercooling. The dark conductivity shows only a slight and momentary drop upon passing through the phase transformation, but the photocurrent for the tetr.- HgI_2 is about two orders of magnitude larger than for the orthorhomb.- HgI_2 . Upon cooling through the transformation point, the change of photosensitivity reverses.

Figure 15(b) shows the temperature variation of the current in the dark and in the light as a function of temperature, for a narrow slit of light illuminating the center of the crystal only, and for nonuniform heating of the crystal so that the phase transformation boundary traveled down the crystal. Any peculiar photosensitive characteristic of the boundary might be expected to indicate itself by a sharp increase in observed photocurrent as the boundary passed through the illuminated region. The curves of Fig. 15(b) do not indicate any such localized sensitivity. The failure to observe such a localized sensitivity may be due simply to the fact that the photocurrents observed even for the slit illumination

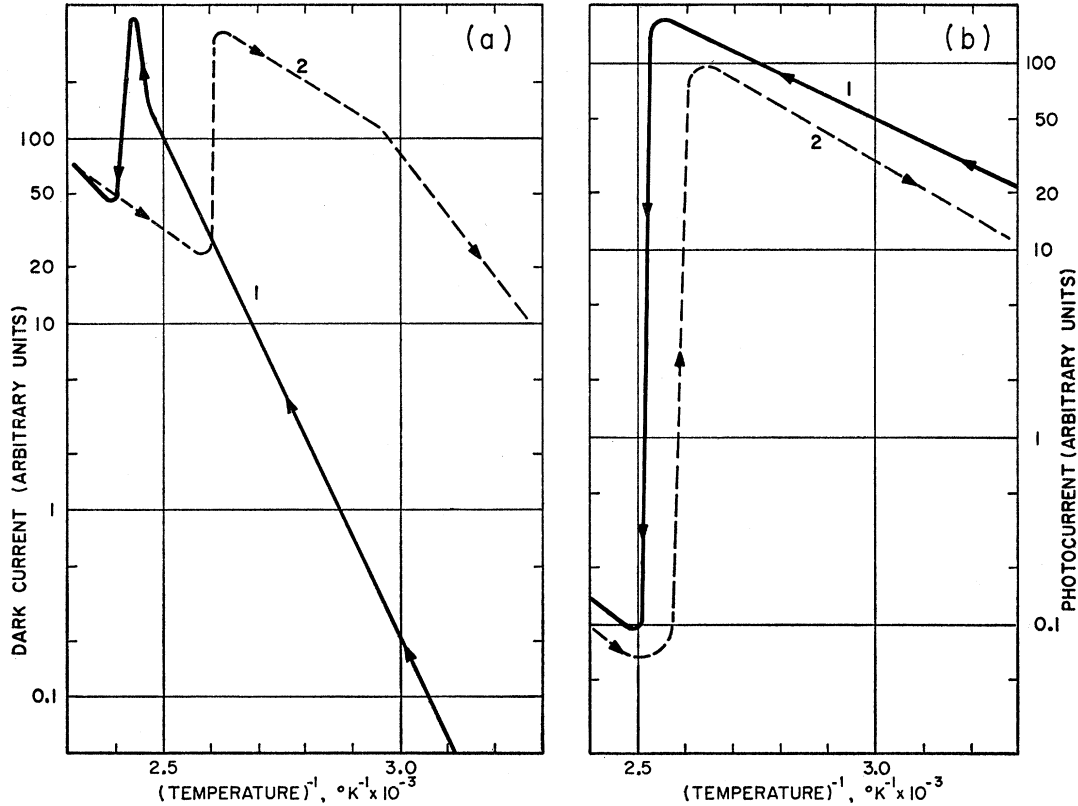


Fig. 16. Temperature variation of dark current (a) and photocurrent (b) through the transformation, for a vapor-phase-grown tetr.-HgI₂ crystal.

are only those generated at the cathode-crystal interface by scattered and diffused light.

10.2. Vapor-Phase-Grown Crystal

Similar effects are found for vapor-phase-grown crystals as for solution-grown crystals, except that the magnitude of the changes in dark conductivity and photoconductivity at the phase transformation are even larger. The curves of Fig. 16 show a change in the dark current of over an order of magnitude and a change in the photocurrent of over three orders of magnitude at the phase transformation. The vapor-phase-grown crystals also show a much larger irreversible increase in dark current as a result of having passed through the phase transformation and undergone partial vaporization.

11. THERMALLY STIMULATED CURRENT

11.1. Analysis of the Measurement

When a crystal is excited at a low temperature so as to fill trapping centers and is then heated in the dark, the measured thermally stimulated current, contributed by electrons freed from traps, in excess of the normal dark current, provides a measure of the density and distribution of trapping centers. Before considering the

experimental data a brief analysis of the method will be given.

The thermally stimulated conductivity, σ_s , will be given by:

$$\sigma_s = n_s e \mu, \quad (1)$$

where n_s is the density of thermally stimulated electrons, given by:

$$n_s = -(dn_i/dt)\tau. \quad (2)$$

n_i is the density of trapped electrons, dn_i/dt is the rate of decrease of the density of trapped electrons, and τ is the lifetime of an electron freed from a trap. The assumption that dn_i/dt may be expressed as:

$$dn_i/dt = -n_i f \exp(-E/kt) \quad (3)$$

leads to an expression for dn_i/dt which may be used in Eq. (2):

$$dn_i/dt = -n_0 f \exp(-E/kt) \times \exp\left[-\int \frac{f}{b} \exp(-E/kt) dt\right]. \quad (4)$$

Here n_0 is the total density of trapped electrons before the beginning of heating, f is the frequency factor for

the thermal release of electrons from traps, E is the trap depth, and b is the heating rate.

We must take account of the following variation of the quantities involved with temperature:

$$f = N_c S v, \quad (5a)$$

$$N_c = N^* T^{\frac{3}{2}}; \quad N^* = 1.9 \times 10^{15}, \quad (5b)$$

$$S = S(T), \quad (5c)$$

$$\tau = \tau(T), \quad (5d)$$

$$\mu = \mu^* T^{-\frac{3}{2}}, \quad (5e)$$

$$v = v^* T^{\frac{1}{2}}; \quad v^* = 5.8 \times 10^5, \quad (5f)$$

where N_c is approximately equal to the density of states in the lowest kT -wide part of the conduction band, S is the capture cross section of the traps, μ is the electron mobility, v is the thermal velocity, and where lattice-scattering only has been assumed.

It is then possible to write the following general equation for the thermally stimulated conductivity:

$$\sigma_s = (n_0 e N^* \mu^* v^*) S(T) \tau(T) T^{\frac{1}{2}} \exp(-E/kt) \times \exp \left[- (N^* v^* / b) \int S(T) T^2 \exp(-E/kT) dT \right]. \quad (6)$$

A maximum value of σ_s will be obtained for $d(\ln \sigma_s)/dT = 0$; i.e.,

$$d(\ln S(T))/dT + d(\ln \tau(T))/dT + d(\ln T^{\frac{1}{2}})/dT + E/(kT^2) - (N^* v^* / b) S(T) T^2 \exp(-E/kT) = 0. \quad (7)$$

The trap depth, E , can then be expressed in terms of the temperature, T_m , at which the maximum thermally stimulated current occurs:

$$E = kT_m \ln \left[\frac{(kN^* v^* / b) S(T_m) T_m^4}{E + kT_m / 2 + [kT_m^2 / \tau(T_m)] (d\tau/dT) + [kT_m^2 / S(T_m)] (dS/dT)} \right]. \quad (8)$$

For $E \gg kT_m / 2$, and for negligible temperature variation of $\tau(T)$ and $S(T)$ for temperatures for which the thermally-stimulated-current curve is obtained, this expression reduces to:

$$E = kT_m \ln [(kN^* v^* / bE) S(T_m) T_m^4]. \quad (9)$$

11.2. Experimental Thermally-Stimulated-Current Data

Thermally-stimulated-current curves for three solution-grown crystals of tetr.-HgI₂, two of which have not passed through a phase transformation and one of which has, and for a tetr.-HgI₂ crystal grown from a solution of 75% HgI₂ and 25% HgCl₂ are shown in Fig. 17. The curve shapes for the crystals grown from solution without HgCl₂ are practically identical, showing three major thermally-stimulated-current maxima. The crystal grown from the solution containing HgCl₂ shows the same current maxima, but with the major peak being the one located near -80°C rather than the one located near 0°C .

The thermally-stimulated-current curves of Fig. 17 indicate that the presence of HgCl₂ in the solution has

TABLE II. Calculated trap parameters.^a

E , ev	T_m , °K	$S(T_m)$, cm ²	$f(T_m)$, sec ⁻¹
0.34	129	6×10^{-13}	10^{13}
0.38	142	6×10^{-13}	10^{13}
0.45	171	2×10^{-13}	7×10^{12}
0.51	196	7×10^{-14}	3×10^{12}
0.59	222	8×10^{-14}	4×10^{12}
0.67	267	7×10^{-15}	6×10^{11}
0.77	293	2×10^{-14}	2×10^{12}

^a Calculated assuming a mobility of 100 cm²/volt sec, and an effective crystal length equal to 1/10 the interelectrode spacing.

had an effect on the relative densities of different types of imperfections formed during the crystal growth; this is in agreement with the presence of much less long-wavelength response (see Fig. 12) for the crystal grown from solution containing HgCl₂ than for the crystals grown from solution not containing HgCl₂.

The trap depths corresponding to the current maxima are listed in Table II, as calculated by determining the location of the electron Fermi-level from the conductivity and the temperature of the current maxima. Using Eq. (9), the values of $S(T_m)$ have been calculated, as well as values of $f(T_m)$ from Eq. (5a). Values of S are large, lying between 10^{-12} and 10^{-14} cm², indicating Coulomb attraction in the trapping process. Corresponding values of f are close to 10^{13} sec⁻¹, the maximum frequency of crystal vibrations. Such values are quite different from those found for CdS, for example, where a trap with depth 0.42 eV and thermally-stimulated-current maximum at -55°C has $S = 7 \times 10^{-18}$ cm² and $f = 3 \times 10^8$ sec⁻¹.

12. PHOTOCURRENT vs VOLTAGE

The evidence discussed previously showing that the photosensitivity of tetr.-HgI₂ is localized at the cathode-crystal junction, suggests that photoconductivity in this case may be related to barrier effects. The presence of barrier effects should become manifest in measurements of the voltage-dependence of photocurrent.

12.1. Room Temperature Data

For many samples it was found that the photocurrent varied as the square-root of the voltage over a considerable voltage range. This variation is demonstrated

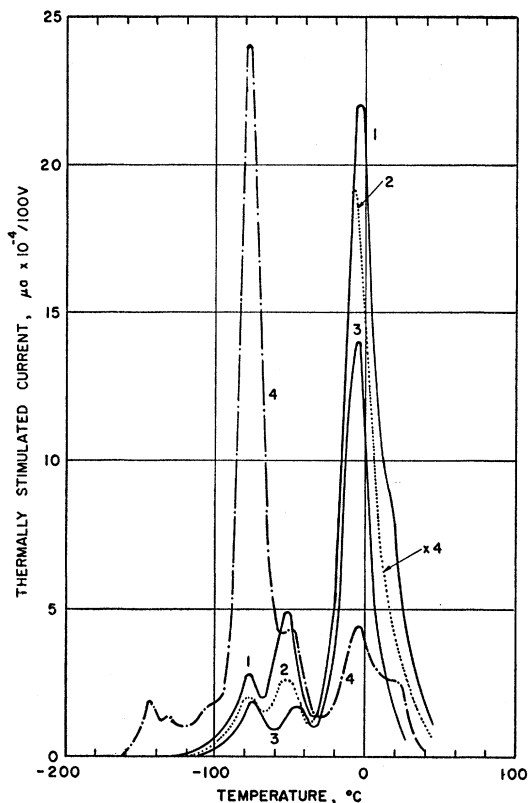


FIG. 17. Thermally stimulated current curves for tetr.- HgI_2 : (1) and (2) solution-grown crystals, (3) same as (1) and (2) after having passed through a transformation cycle, (4) solution-grown crystal from solution containing 25% HgCl_2 .

for the sintered layer of tetr.- HgI_2 in Fig. 18. The photocurrent as a function of voltage is shown for nine different light intensities and the slope of the curves are shown for each light intensity. All slopes are close to 0.5 over the whole range of voltage. The dark current, on the other hand, is approximately linear with voltage. A similar set of data for a solution-grown crystal is shown in Fig. 19. Here measurements at low voltages, below about 1 to 5 volts, show an approximately linear variation of photocurrent with voltage, breaking into the near-square-root variation for higher voltages. Exactly similar curves are obtained for reversed polarity of the applied field.

Such variations of photocurrent with the square-root of the light intensity are not limited to samples with graphite electrodes. Insofar as measurements with Ag, Ga, and In electrodes were possible, similar phenomena were found.

12.2. Temperature Dependence

The temperature dependence of the photocurrent-voltage characteristic for four different types of tetr.- HgI_2 is shown in Fig. 20. In this figure, the slope of the log-log plot of photocurrent *vs* voltage, for voltages above 10 volts, is shown as a function of temperature.

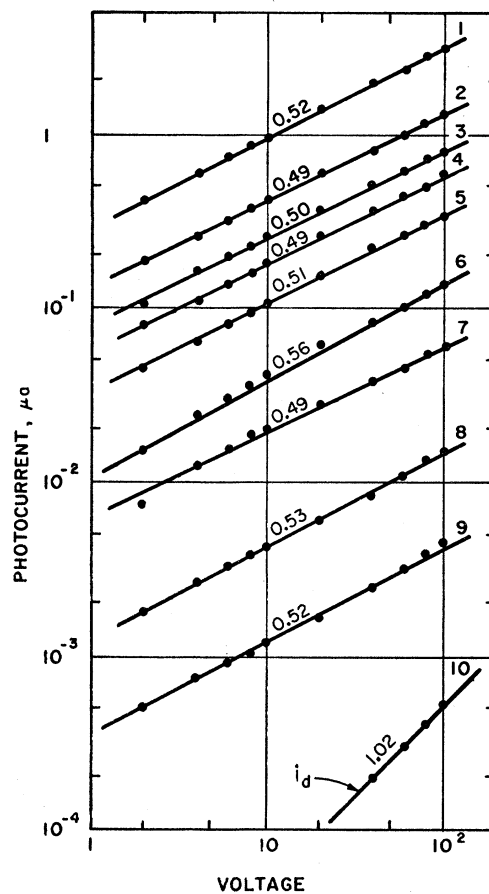


FIG. 18. Photocurrent as a function of voltage for a sintered layer of tetr.- HgI_2 at room temperature at different light intensities: (1) 180 ft-c, (2) 62 ft-c, (3) 39 ft-c, (4) 26 ft-c, (5) 13 ft-c, (6) 4.8 ft-c, (7) 1.9 ft-c, (8) 0.29 ft-c, (9) 0.043 ft-c, (10) dark.

(Below 10 volts, some rather complicated variations of photocurrent with voltage were found at different temperatures, the simplest behavior being exhibited by the melted-and-recrystallized layer and the vapor-phase-grown crystal which showed substantially the same variation between 1 and 100 volts.) Figure 20 indicates that for all the samples, a near-linear variation of photocurrent with voltage is found at temperatures below 0°C , which changes rapidly into a near-square-root variation of photocurrent with voltage above 0°C .

When the electric field applied to a barrier, such as a Schottky-type exhaustion barrier, is sufficiently large to sweep the photoexcited holes out of the barrier, saturation of photocurrent with field occurs. The square-root variation of photocurrent with voltage found in HgI_2 may be interpreted as such a saturation process with some variation of barrier height or width with applied field so that complete saturation does not occur. It is questionable whether too much importance should be attributed to the exact "square-root" nature of the variation, for Figs. 19 and 20 show that powers between 0.37 and 0.74 have been observed.

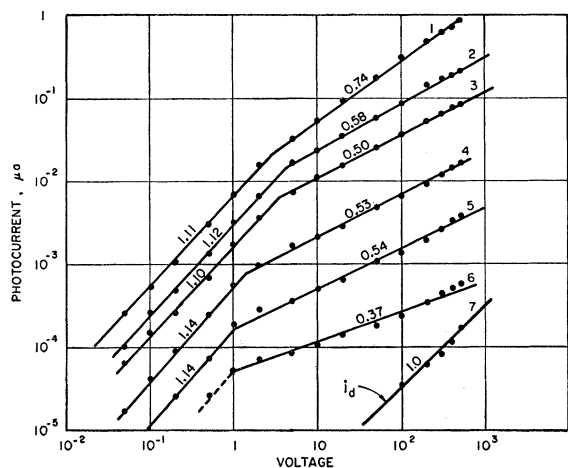


FIG. 19. Photocurrent as a function of voltage for a solution-grown tetr.- HgI_2 crystal at room temperature at different light intensities: (1) 900 ft-c, (2) 330 ft-c, (3) 130 ft-c, (4) 20 ft-c, (5) 3.0 ft-c, (6) 0.47 ft-c, (7) dark.

The width of a Schottky-type exhaustion layer²⁷ for example, varies as $N^{-\frac{1}{2}}$, where N is the density of localized positive charges in the barrier layer. N will be a function of temperature and will be small at low temperatures, giving a large barrier width, which in turn will require a higher field to produce saturation. As temperature increases, N will increase until finally the temperature is reached where the saturation effect is observable in the voltage range investigated. Thus the

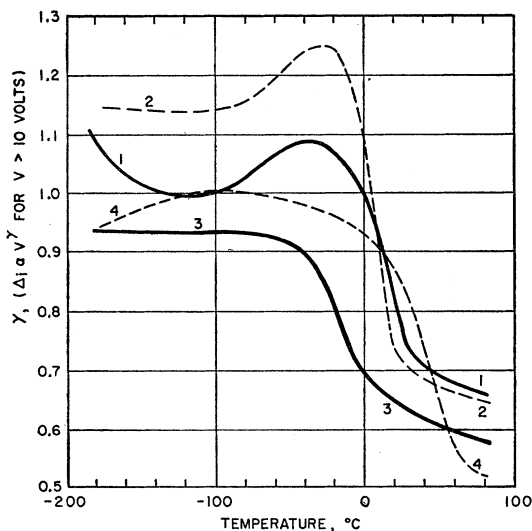


FIG. 20. Slope of the log-log plot of photocurrent vs voltage for voltages greater than 10 volts, as a function of temperature for tetr.- HgI_2 : (1) solution-grown crystal, (2) same as (1) after having passed through a transformation cycle, (3) melted-and-recrystallized layer, (4) vapor-phase-grown crystal.

²⁷ See, for example, C. Kittel, *Introduction to Solid State Physics* (John Wiley and Sons, Inc., New York, 1956), second edition, p. 388.

variation indicated in Fig. 20 agrees with the general picture.

13. PHOTOCURRENT vs LIGHT INTENSITY

The spectral response curves of Fig. 13 showed that a maximum photocurrent was observed at a certain temperature for solution-grown crystals for excitation by wavelengths equal to or greater than the absorption edge. Since a maximum photocurrent implies the presence of temperature-quenching of photoconductivity at temperatures above the maximum, the de-

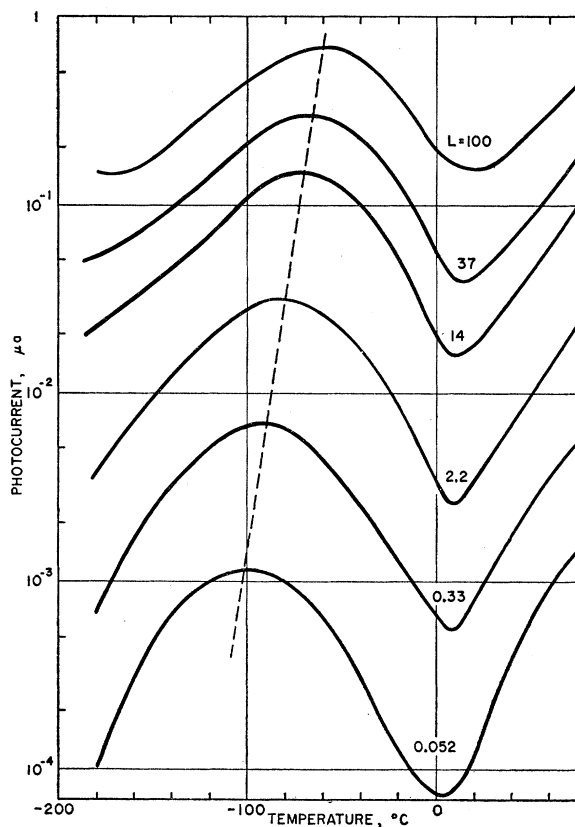


FIG. 21. Photocurrent as a function of temperature for different light intensities for a solution-grown tetr.- HgI_2 crystal; applied voltage of 100 volts; $L=100$ corresponds to 900 ft-c.

pendence of the location of the photocurrent maximum with light intensity was investigated to see if the phenomena could be treated by the same model shown to be successful for CdS and CdSe.²⁸

Figure 21 shows the variation of photocurrent with temperature for several different light intensities (incandescent source) for a solution-grown crystal. A pronounced maximum occurs which shifts from about -60° to -102°C as the light intensity is lowered by a factor of about 2000. A minimum photocurrent is found at about 0°C , followed by a rise which has been pre-

²⁸ R. H. Bube, *J. Phys. Chem. Solids*, **1**, 234 (1957).

viously pointed out (see Figs. 15 and 16). Such behavior occurs for solution-grown crystals whether or not they have passed through a transformation. It is not found, however, for crystals grown from the vapor phase or for a melted-and-recrystallized layer. Typical curves for a melted-and-recrystallized layer are given in Fig. 22, which show only the slightest trace of a maximum; curves obtained for a vapor-phase-grown crystal showed even less indication of a photocurrent maximum. It was pointed out in connection with Fig. 13, that a maximum photocurrent as a function of temperature was not found for excitation by wavelengths shorter than the absorption edge, but only for wavelengths equal to or longer than the absorption edge. This fact explains the

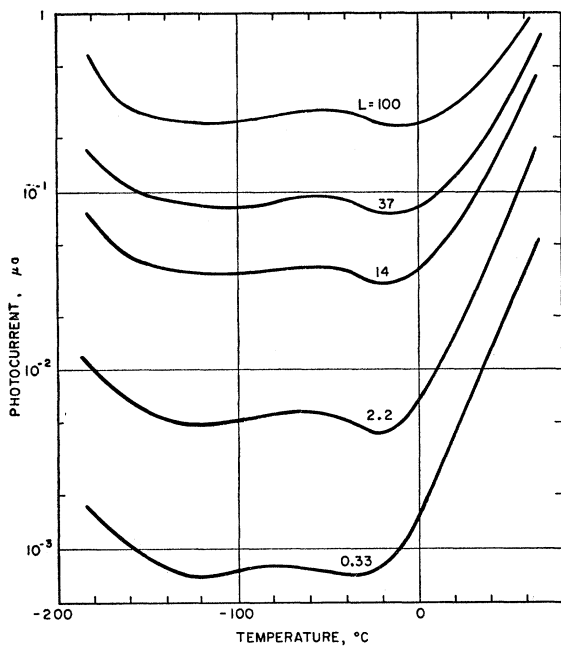


FIG. 22. Photocurrent as a function of temperature for different light intensities for a melted-and-recrystallized layer of tetr.-HgI₂; applied voltage of 100 volts; $L=100$ corresponds to 900 ft-c.

differences in temperature behavior and correlates them with the spectral response curves: (1) most of the sensitivity for the vapor-phase-grown crystals and the melted-and-recrystallized layer comes from wavelengths shorter than the absorption edge (see Figs. 12 and 14), whereas (2) most of the sensitivity for the solution-grown crystals comes from wavelengths equal to or greater than the absorption edge (see Figs. 12 and 13). It may be concluded that the centers responsible for the photocurrent maximum are volume centers only and that their incorporation is the result of growth from solution.

The curves of Fig. 21 are all for an applied voltage of 100 volts. If the dependence of the photocurrent *vs* temperature curve is examined at constant light intensity but at several voltages, the results of Fig. 23

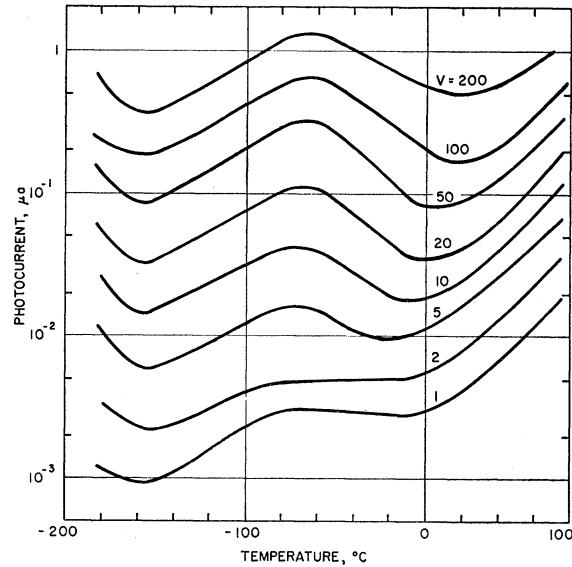


FIG. 23. Photocurrent as a function of temperature for different voltages for a solution-grown crystal of tetr.-HgI₂; light intensity of 900 ft-c.

are obtained. For very small voltages, the photocurrent maximum is practically absent, not because there is no rise in photocurrent at low temperatures, but because there is no dip in photocurrent at intermediate temperatures before the high-temperature rise. The maximum is found for all voltages above 5 volts, however. It is concluded that its absence at low voltages is the result of a complex photocurrent-voltage-temperature relationship, and that the maximum does indicate a fundamental characteristic of the material.

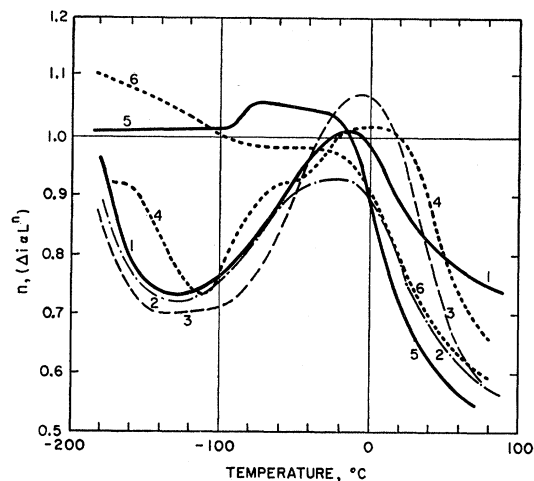


FIG. 24. Slope of the log-log plot of photocurrent *vs* light intensity (over the range of 900 to 0.5 ft-c) as a function of temperature for tetr.-HgI₂: (1) and (2) solution-grown crystals, (3) same as (1) and (2) after having passed through a transformation cycle, (4) solution-grown crystal from solution containing 25% HgCl₂, (5) melted-and-recrystallized layer, (6) vapor-phase-grown crystal. Applied voltage of 100 volts.

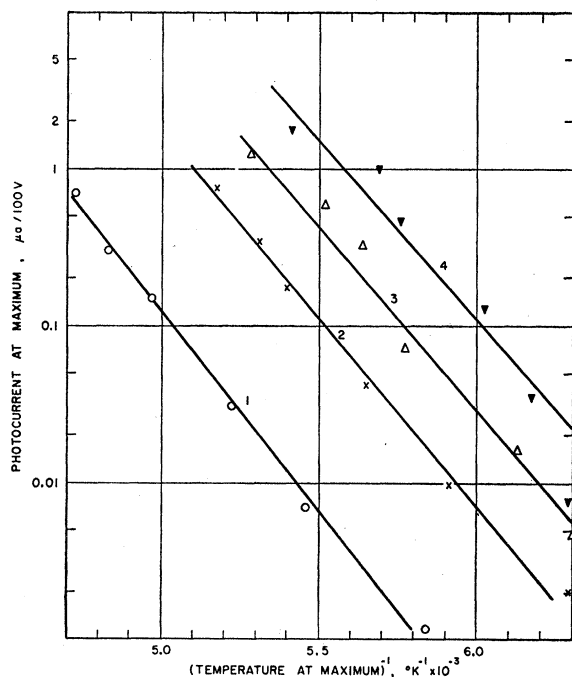


Fig. 25. Log of the photocurrent at the maximum as a function of the reciprocal temperature at the maximum for different light intensities for tetr.-HgI₂: (1) and (2) solution-grown crystals, (3) same as (1) and (2) after having passed through a transformation cycle, (4) solution-grown crystal from solution containing 25% HgCl₂.

Further information can be obtained by considering the temperature dependence of the variation of photocurrent with light intensity. Assuming photocurrent proportional to the n th power of the light intensity, Fig. 24 is a plot of n as a function of T for six different samples of tetr.-HgI₂. The samples can be immediately separated into two types: (1) those that have a photocurrent maximum also show a maximum in n at temperatures to the high side of the photocurrent maximum; and (2) those that do not have a photocurrent maximum show approximately constant n up to about 0°C. Following the variation of n with temperature for Curves 1 through 4 of Fig. 24, we see that the low temperature increase in photocurrent with temperature is accompanied by a decrease in n from near 1.0 to about 0.7, the decrease in photocurrent past the photocurrent maximum is accompanied by an increase in n from 0.7 to about 1.0, and the high temperature increase in photocurrent with temperature is accompanied by a decrease in n from 1.0 to values between 0.5 and 0.7.

An increase of photocurrent with temperature is usually the result of the change-over of certain centers with levels near the conduction band from the role of recombination centers to the role of trapping centers. One case is that in which the density of electrons trapped above the steady-state electron Fermi-level is greater than that trapped below; for a uniform distribution of trapping centers, such a model predicts an exponential

variation of photocurrent with reciprocal temperature and a variation of photocurrent with the square-root of light intensity.²⁹ Such a variation has indeed been observed for CdSe²⁸ and for ZnTe.³⁰ The high temperature variation of photocurrent for tetr.-HgI₂ also seems to follow this type of mechanism. A similar mechanism in a different range may be assumed for the increase of photocurrent with temperature below the photocurrent maximum in solution-grown crystals.

The model of temperature quenching discussed in a previous publication²⁸ for CdS and CdSe showed that temperature quenching was accompanied by a photoconductivity which varied more rapidly than linearly with light intensity. n was of the order of unity below the region of temperature quenching and became greater than unity in the region of temperature quenching. It may simply be shown, however, that the same model predicts that temperature quenching will be accompanied by an increase in n from near 0.5 to near 1.0 (instead of from near 1.0 to greater than 1.0) under a number of other possible boundary conditions, such as either the presence of shallow traps lying very near the conduction band or a very low density of any traps empty in the dark, much less than the density of recombination centers.

In accord with the previous model, the photocurrent maximum corresponds to a location of the hole demarcation level for low-lying centers (with capture cross section for electrons smaller than that for holes) being at the energy level corresponding to the centers. The mechanism of temperature quenching involves the transfer of holes from these small capture cross section

TABLE III. Calculated parameters for the "sensitizing" centers.

Crystal	Distance of "sensitizing" centers above valence band, ev	Ratio of cross section for holes to that for electrons for "sensitizing" centers ^a
Solution-grown; has not passed through transformation	0.54	9×10^2
Solution-grown; has not passed through transformation	0.52	7×10^3
Solution-grown; has passed through transformation	0.46	3×10^2
Solution-grown; from solution with 25% HgCl ₂ , has not passed through transformation	0.51	7×10^4

^a Calculated assuming an effective crystal length equal to 1/10 the interelectrode spacing.

²⁹ A. Rose, RCA Rev. **12**, 362 (1951).

³⁰ R. H. Bube and E. L. Lind, Phys. Rev. **105**, 1711 (1957).

(for electrons) centers to other recombination centers with a larger cross section for electrons. It has been shown that the following condition holds:

$$\ln n_m = \ln(N_v S/S') - E^*/kT_m, \quad (10)$$

where n_m is the density of free electrons at the photocurrent maximum, N_v is approximately equal to the density of states in the upper kT -wide part of the valence band, S is the capture cross section of the low-lying "sensitizing" centers for holes, S' is the capture cross section of the low-lying "sensitizing" centers for electrons, E^* is the height of the energy level corresponding to these centers above the valence band, and T_m is the temperature of the photocurrent maximum.

The logarithm of the photocurrent at the maximum is plotted in accord with Eq. (10) as a function $1/T_m$ in Fig. 25, for four different samples of tetr.-HgI₂. Values of E^* and S/S' obtained from the data of Fig. 25 are summarized in Table III. All the data indicate a level about 0.5 eV above the valence band for the "sensitizing" centers. Calculated values of S/S' show considerable variation; the determination of S/S' however requires the calculation of n_m which will depend on the length of the crystal which is actually taking part in the photoconductivity process. It is not surprising therefore, that the agreement in the calculations of S/S' is much poorer than in those of E^* .

Table IV summarizes values of E^* , T_m , S/S' , and specific sensitivity for CdSe, ZnTe, and HgI₂. Fair agreement is found between E^* and T_m , and between S/S' and the specific sensitivity, especially since neither relationship is a direct one: for fixed E^* and n_m , T_m will vary with the value of S ; specific sensitivity depends very strongly on the value of the capture cross section for electrons of the large-cross-section recombination centers, which need not have any direct relationship with the value of S .

14. SUMMARY

Photoconducting HgI₂ has been prepared in crystal form from solution and from vapor phase growth, and also in sintered and melted-and-recrystallized layer form.

Tetr.-HgI₂ has a band-gap of 2.11 eV at room temperature; at 400°K, the tetragonal form transforms to the orthorhomb.-HgI₂ which has a band-gap of 2.31 eV at 400°K.

Tetr.-HgI₂ has a temperature coefficient for band-gap

TABLE IV. Summary of crystal characteristics.

Material	E^* , eV	T_m , °C	S/S'	Specific sens., mho cm ² /watt
CdSe	0.64	0	10 ⁶	10 ⁻¹
ZnTe	0.34	-120	10	10 ⁻⁵
HgI ₂	0.51	-80	10 ³	10 ⁻⁵

variation of -7×10^{-4} eV/degree between 100° and 200°K and of -14×10^{-4} eV/degree between 330 and 400°K. Orthorhomb.-HgI₂ has a temperature coefficient of -24×10^{-4} eV/degree for band-gap variation between 90° and 200°K, which extrapolates to the measured band-gap at 400°K. This latter temperature coefficient is some 3 to 8 times larger than temperature coefficients previously reported for many materials.

The photosensitivity of the tetr.-HgI₂ crystals was confined to a small portion of the crystal near the cathode. Dependence of photocurrent on voltage is interpreted in terms of a barrier at the cathode; the sweeping of photoexcited holes out of the barrier produces saturation effects, the temperature dependence of which is consistent with the barrier interpretation.

The measurement of dark current and photocurrent as the HgI₂ passes through the phase transformation from tetragonal to orthorhombic, shows a small drop in dark current and a much larger drop in photocurrent (up to three orders of magnitude). The variation in photocurrent is reversible upon producing the transformation in the reverse direction, even though the crystallinity of the sample has been effectively destroyed.

An analysis of thermally stimulated current data indicates the presence of Coulomb-attraction in trapping processes in HgI₂, with capture cross sections up to 6×10^{-13} cm² being found. The corresponding frequency factor is 10^{13} sec⁻¹, equal to the highest crystal vibration frequency.

Investigation of a photocurrent-*vs*-temperature maximum for solution-grown crystal indicates that it is associated with the presence of low-lying "sensitizing" centers (0.5 eV above the valence band) which are present in the volume of the crystal only. The effects are describable in terms of the same model as that used previously for CdS, CdSe, and ZnTe.

The author wishes to express his appreciation to Dr. R. E. Shrader for his assistance in making the measurements on diffuse reflectivity and luminescence emission, to Dr. S. M. Thomsen for preparation of samples, and to M. A. Lampert for helpful discussions.

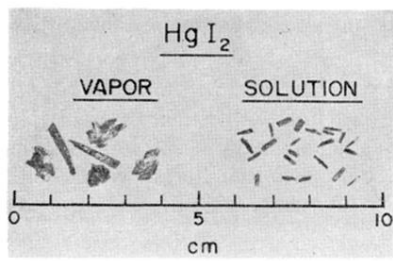


FIG. 1. Photograph of HgI_2 crystals grown from the vapor-phase and from acetone solution.